Green-Synthesized SeO/ZnO Nanocomposites from *Musa acuminata* Peel: Implications for Anticancer and Antimicrobial Strategies in Public Health

Nada H. Aljarba,[a] Hamida Hamdi,[b,c] Luluah M. Al Masoudi,[b] Noha T. Al Thagafi,[b] Ashwaq T. Althobaiti,[b] Dalal M. Alkuraythi,[d] Dina A. Altwiley,[d] Adil Abalkhail,[e] and Mohamed K. Y. Soliman [f,*]

An eco-friendly one-pot approach was employed to biosynthesize selenium oxide/zinc oxide (SeO/ZnO) nanocomposites using banana peel (*Musa acuminata* L.) extract. The phytogenic nanocomposite was characterized using FTIR, UV–Vis spectroscopy, TEM, SEM, and EDX analyses. A distinct absorbance peak at 336 nm confirmed nanocomposite formation, while FTIR results indicated the involvement of plant phytochemicals in stabilization and surface functionalization processes. TEM images revealed quasi-spherical nanoparticles with an average diameter of 64 nm. Elemental analysis (EDX) confirmed the presence of selenium and zinc, suggesting that selenium is predominantly present in oxide form (SeO) within the ZnO matrix. Biological evaluations showed significant multifunctional activity. The SeO/ZnO nanocomposite exhibited selective antiproliferative activity against A549 lung cancer cells (IC_{50} = 100.9 µg/mL) compared to normal Vero cells (IC_{50} = 263.5 µg/mL), indicating favorable selectivity. Pronounced antibacterial activity was observed, particularly against *Bacillus subtilis* (MIC = 62.5 µg/mL; inhibition zone = 27.8 ± 0.75 mm). Concentration-dependent antioxidant activity was confirmed using DPPH and ABTS assays, with IC_{50} values of 256.8 and 339.40 µg/mL, respectively.

DOI: 10.15376/biores.21.2.5010-5023

Keywords: SeO/ZnO NCs; Green synthesis; Anticancer activity; Antibacterial activity; Antioxidant activity

Contact information: a: Department of Biology, College of Science, Princess Nourah bint Abdulrahman University, P.O. Box 84428, Riyadh 11671, Saudi Arabia; b: Department of Biology, College of Science, Taif University, P.O. Box 11099, Taif 21944, Saudi Arabia; c: Zoology Department, Faculty of Science, Cairo University, Giza 12613, Egypt; d: Department of Biological Sciences, University of Jeddah, Jeddah, Saudi Arabia; e: Department of Public Health, College of Applied Medical Sciences, Qassim University, P.O. Box 6666, 51452 Buraydah, Saudi Arabia; f: Botany and Microbiology Department, Faculty of Science, Al-Azhar University, Nasr City 11884, Cairo, Egypt;
**Corresponding author: Mohamed.k.yousef@azhar.edu.eg*

INTRODUCTION

The rapid emergence of antimicrobial resistance, increasing cancer incidence, and oxidative stress-related disorders has intensified the search for multifunctional nanomaterials with enhanced biological performance (Soliman *et al*. 2024; Abdelghany *et al*. 2019). Nanotechnology offers unique opportunities to engineer materials with tunable physicochemical properties, high surface reactivity, and improved biological interactions (Abu-Elghait *et al*. 2025). Across different metal oxide nanoscale materials, ZnO

nanoparticles have attracted considerable attention owing to their wide band gap, chemical stability, biocompatibility, and broad-spectrum antimicrobial and anticancer activities. The observed bioactivity can be attributed to enhanced ROS generation, controlled Zn^{2+} ion release, and efficient surface-mediated cellular interactions (Kadhim *et al*. 2025).

To further enhance the functional efficiency of ZnO nanoparticles, incorporation of selenium-based oxide species such as selenium oxide (SeO) has emerged as a promising strategy (Qanash *et al.* 2024). Selenium oxide is known for its redox-active properties, enabling effective modulation of oxidative stress, along with notable antimicrobial and antioxidant activities (Lashin *et al*. 2023). At the nanoscale, selenium-containing oxide nanostructures exhibit improved surface reactivity and enhanced interaction with biological systems. In addition, SeO–ZnO nanocomposites have demonstrated enhanced antibacterial and antioxidant performance; this was attributed to synergistic interactions between ZnO and selenium oxide species, leading to increased ROS generation and improved cellular targeting (Qanash *et al.* 2024). Moreover, surface-active electrons present on the nanoparticles are capable of pairing with the unpaired electrons of free radicals, thereby stabilizing them and exhibiting antioxidant properties (Rahman *et al*. 2021).

Although conventional physical and chemical approaches enable the rapid production of nanoparticles in large amounts, the reliance on toxic chemical reducing and stabilizing agents can result in serious and irreversible environmental hazards (Upadhyay *et al*. 2015; Abu-Dalo *et al*. 2019). The growing intensity of environmental challenges has created an urgent need for safer and more sustainable green methods for NP synthesis (Abdelhady *et al*. 2024; Majeed *et al.* 2020). Recently, plant extracts have gained attention functioning as biogenic reducing and surface-stabilizing agents in the preparation of nanoparticles. The green synthesis of different metal and metal oxide NPs using various plant extracts has been widely documented (Alikhani *et al*. 2022). These plant sources are typically abundant in phenolic compounds and various phytochemical constituents in addition to minerals, which can interact with metal ions during the reaction, promoting nanoparticle formation and enhancing their stability (Soliman *et al*. 2025; Soliman and Salem 2025; Saied *et al*. 2025). Phytomediated synthesis avoids the use of hazardous chemicals and eliminates the complex microbial cultivation steps required in other green biotechnological methods, such as microbe-assisted synthesis, making it more practical and suitable for large-scale production (Selim *et al*. 2025; Abdelghany *et al*. 2018).

Banana peels are considered a rich source of nutrients, containing about 50% dietary fiber on a dry weight basis, in addition to nearly 7% protein and several essential amino acids (Emaga *et al*. 2007). They also include considerable amounts of organic components such as carbohydrates, fats, and proteins, which makes them an important source of carbohydrates. The high fiber content in banana peels contributes to relieving constipation and supporting overall health and well-being. In addition, banana peels are abundant in phytochemical compounds; these biomolecules contribute primarily to colloidal stability and surface functionalization rather than acting as strong reducing agent (Nguyen *et al.* 2003; Someya *et al.* 2002).

To the best of the authors' knowledge, this is the first study to report the green one-pot synthesis of SeO/ZnO nanocomposites using *Musa acuminata* peel extract, combined with comprehensive physicochemical characterization and systematic evaluation of multifunctional biological activities. In light of these considerations, this study aimed to synthesize a SeO/ZnO nanocomposite using a green approach based on *Musa acuminata* peel extract, followed by comprehensive physicochemical characterization. Additionally,

the biological activities of the synthesized nanocomposite, including anticancer, antibacterial, and antioxidant properties, were systematically investigated.

EXPERIMENTAL

Material

Analytical-grade chemicals besides reagents were used throughout the study and were commercially acquired from Sigma–Aldrich (St. Louis, MO, USA) including sodium selenite (Na_2SeO_3), zinc nitrate hexahydrate [$Zn(NO_3)_2 \cdot 6H_2O$], dimethyl sulfoxide (DMSO), methanol, Mueller–Hinton (M–H) agar, glacial acetic acid, sodium hydroxyl (NaOH), hydrochloric acid (HCl), and crystal violet. Fresh banana fruits (*Musa acuminata* L.) were obtained from a local market and used for peel extract preparation.

Green One-Pot Bio-fabrication of SeO/ZnO Nanocomposite

Fresh peels of ripe *Musa acuminata* L. were collected, washed thoroughly with tap and distilled water, cut into small pieces, and air-dried for 5 to 7 days. After that they were oven-dried at 50 to 60 °C until constant weight. Following drying, the peels were processed into a fine particulate powder and preserved under airtight condition. To prepare the extract, 10 g of peel powder was mixed with 100 mL distilled water, heated at 70 to 80 °C for 20 to 30 min with stirring, cooled, filtered, and stored at 4 °C. The extract was filtered using Whatman No. 1 filter paper, and the filtrate was collected for green one-pot synthesis of the SeO/ZnO nanocomposite. Then, 0.1 M zinc nitrate hexahydrate and 1 mM sodium selenite were dissolved in distilled water at 70 °C under stirring. The banana peel extract was added dropwise, and the pH was adjusted to 10 using 1 M NaOH to facilitate ZnO formation and enable the interaction of selenium species with the ZnO matrix. The reaction was maintained for 2 h until precipitate formation. The product was collected by centrifugation (10,000 rpm, 15 min), washed with water and ethanol, dried at 80 °C overnight, and calcined at 400 °C for 2 h to obtain crystalline SeO/ZnO nanocomposite powder.

Characterization

The bio-fabricated SeO/ZnO nanocomposite was characterized using several physicochemical techniques. UV–visible spectroscopy (JASCO V-730 double-beam) was used to assess optical properties and verify nanocomposite formation, with spectra recorded from 200 to 800 nm. Morphology, particle size, and structural characteristics were examined by TEM (JEOL JEM-1010); a drop of nanoparticle suspension was placed on a carbon-coated copper grid, air-dried, and excess solution was removed before imaging. FTIR analysis (JASCO FTIR-6100) was conducted to identify functional groups involved in stabilization and surface functionalization of the nanocomposite. Dried samples were mixed with KBr, pelletized, and scanned between 400 and 4000 cm^{-1}. Surface morphology was further evaluated by SEM (ZEISS EVO-MA 10, Germany), while elemental composition and the presence of Se and Zn were confirmed using EDX (BRUKER Nano GmbH, Germany) (Khormi *et al*. 2025).

Anticancer and Cytotoxicity

The cytotoxic and anticancer activities of the SeO/ZnO nanocomposite were investigated using the MTT (3-(4,5-dimethylthiazol-2-yl)-2,5-diphenyltetrazolium

bromide) colorimetric assay on normal African green monkey kidney cells (Vero) and human lung adenocarcinoma cells (A549). Cells were maintained in Dulbecco's Modified Eagle Medium (DMEM) supplemented with 10% fetal bovine serum (FBS), 100 µg/mL streptomycin, and 100 U/mL penicillin. The mixture was incubated at 37 °C in a humidified atmosphere with 5% CO_2. Cultures were allowed to reach approximately 80 to 90% confluence before treatment. For the assay, cells were seeded into 96-well plates at a density of 1×10^5 cells/mL and incubated for 24 h to ensure proper attachment. The culture medium was then replaced with 100 µL of fresh medium containing different concentrations of the SeO/ZnO nanocomposite (15.78 to 1000 µg/mL). Cells treated with medium only were used as the negative control. After 72 h of incubation under standard conditions, MTT solution was added to each well and incubated for 2 to 4 h at 37 °C. Metabolically active cells reduced the yellow MTT reagent into insoluble purple formazan crystals. The formed crystals were dissolved in DMSO. The optical density was measured at 570 nm using a microplate reader as an indicator of cell viability.

In Vitro Antibacterial Activity and Determination of MIC and MBC of SeO/ZnO Nanocomposite

The antimicrobial activity of the synthesized SeO/ZnO nanocomposite was estimated using the agar well diffusion technique counter to *Escherichia coli*, *Klebsiella pneumoniae*, and *Bacillus subtilis*. Briefly, standardized bacterial suspensions (10^8 CFU/mL) were spread onto nutrient agar plates, and wells (6 mm diameter) were filled with 100 µL of the nanocomposite solution. Gentamicin was used as a positive control, while DMSO served as a negative control. After incubation at 37 °C for 24 h, antibacterial activity was assessed by measuring the inhibition zone diameters. The minimum inhibitory concentration (MIC) was determined using the broth microdilution method according to CLSI guidelines, with serial two-fold dilutions prepared in Mueller–Hinton broth and inoculated with ~5×10^5 CFU/mL bacterial suspensions. The MIC was defined as the lowest concentration that completely inhibited visible growth after 24 h of incubation. The minimum bactericidal concentration (MBC) was determined by subculturing aliquots from the MIC and higher concentrations onto Mueller–Hinton agar plates and was defined as the lowest concentration resulting in ≥99.9% reduction in bacterial growth.

Antioxidant Assays

DPPH radical scavenging activity

The antioxidant potential of the SeO/ZnO nanocomposite was determined using the DPPH free radical scavenging assay. A 1 mM DPPH solution was prepared in 50% methanol and kept in the dark at room temperature for 30 min before use. Various concentrations of the nanocomposite (25 to 1000 µg/mL) were added to the DPPH solution and incubated in the dark for 30 min at room temperature. Ascorbic acid was used as a positive control, while DPPH solution without the nanocomposite served as a negative control. The reduction in absorbance was recorded at 517 nm using a UV–visible spectrophotometer, and the radical scavenging activity was calculated accordingly.

ABTS radical scavenging activity

The antioxidant activity was further evaluated using the ABTS radical cation decolorization assay. The $ABTS^{\bullet+}$ radical was generated by mixing 7 mM ABTS with 2.4 mM potassium persulfate and incubating the mixture in the dark at 25 °C for 12 to 16 h. The resulting solution was diluted with ethanol (1:89, v/v) to obtain a suitable absorbance.

Equal volumes (1 mL) of diluted ABTS solution and different concentrations of the SeO/ZnO nanocomposite (25 to 1000 µg/mL) were mixed and incubated at room temperature for 10 min. Ascorbic acid served as a positive control, while ABTS solution without the nanocomposite was used as a negative control.

Statistical Evaluation

Data (mean ± SD, n = 3) were analyzed using one- or two-way ANOVA with Tukey's HSD test at $P < 0.05$ (OriginPro 18.0).

RESULTS AND DISCUSSION

Characterization

The UV–visible absorption spectrum of the integrated SeO/ZnO nanocomposite revealed a peak at 336 nm (Fig. 1a). This was consistent with the fact that its characteristic excitonic absorption typically appears in the UV region. This shift may be associated with several synergistic factors. First, nanoscale size reduction may induce quantum confinement effects, leading to band-edge modulation. Second, and more importantly, the interaction of selenium species with the ZnO system or at the ZnO interface can alter the local electronic environment. Selenium incorporation is known to introduce defect-mediated energy states or modify oxygen vacancy concentration, which directly influences the optical transition probability and band structure. The surface plasmon resonance (SPR) behaviour is strongly influenced by nanoparticle characteristics such as particle size, geometric shape, surface morphology, crystallinity, and surrounding dielectric environment (Adrianto *et al*. 2022). Variations in these physicochemical parameters significantly affect the optical response and absorption features observed in UV–Vis spectroscopy. Comparable colour transitions and characteristic absorption bands have been documented in earlier reports during nanoparticle formation. For example, biosynthesized ZnSe nanoparticles prepared using seaweed extract demonstrated distinct absorbance bands around 250 and 360 nm, confirming nanoparticle generation and their specific optical properties (Mirzaei *et al*. 2021).

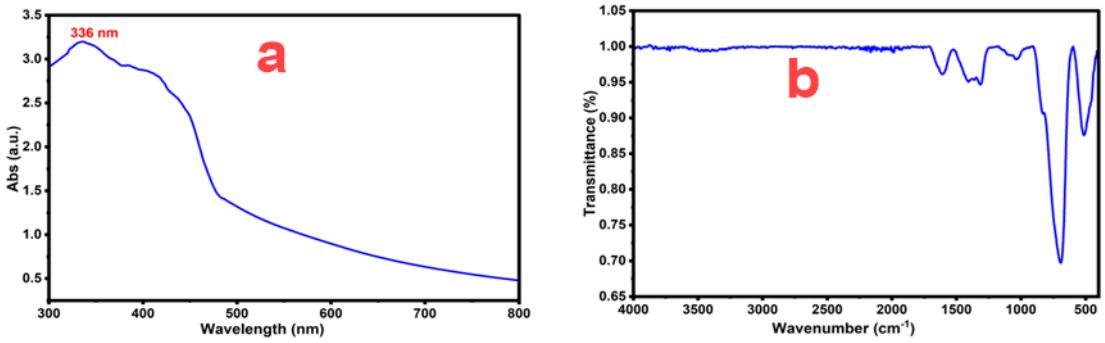

Fig. 1. UV–visible (a) and FTIR (b) spectra of green-synthesized SeO/ZnO nanocomposite

The FTIR spectral profile (400 to 4000 cm^{-1}) of the biogenically synthesized SeO/ZnO nanocomposite confirmed its structural formation and the involvement of banana peel phytochemicals in stabilization and surface functionalization processes (Fig. 1b). A broad absorbance band observed around 3515 to 3340 cm^{-1} is attributed to O–H stretching

vibrations of hydroxyl groups, indicating the presence of phenolic compounds and adsorbed water molecules (Meenakshi *et al*. 2024). The peak detected at approximately 1608 cm^{-1} corresponds to C=O stretching or aromatic C=C vibrations, suggesting the contribution of polyphenols and flavonoids from the banana peel extract in nanoparticle stabilization. Bands appearing at 1407 to 1362 cm^{-1} are associated with C–N stretching and O–H bending vibrations of biomolecules. The absorbance band around 1033 cm^{-1} is assigned to C–O stretching vibrations of alcohols, ethers, or ester functional groups, confirming the interaction between phytochemicals and the nanoparticle surface (Pasieczna-Patkowska *et al.* 2025). Importantly, strong characteristic bands observed at 693 and 512 cm^{-1} correspond to Zn–O stretching vibrations, confirming the formation of ZnO crystalline structure (Ruiz-Duarte *et al*. 2025).

The TEM micrograph (Fig. 2a) revealed the formation of quasi-spherical nanoparticles with noticeable aggregation. The particles were relatively well-dispersed but exhibited partial clustering, which may be attributed to high surface energy and interparticle interactions at the nanoscale. The particle size distribution histogram (Fig. 2b) demonstrated a mean particle diameter of about 64 nm, indicating moderate polydispersity. The size range (35 to 110 nm) suggests controlled nucleation followed by growth and partial coalescence during synthesis. Nearly nanoscale distributions have been reported for ZnO-based nanocomposites synthesized *via* green routes (Al-Rajhi *et al*. 2022). The observed size regime is particularly significant, as nanoscale SeO/ZnO NCs below 100 nm often exhibit enhanced surface-to-volume ratios, leading to improved biological properties (Anitha *et al*. 2025). The SEM image (Fig. 2c) exhibits a coarse and non-uniform surface morphology with aggregated granular structures. The existence of compact clusters suggests strong interparticle adhesion, which is common in ZnO-based nanostructures due to their intrinsic polarity and high surface reactivity. Surface roughness and porous texture may enhance active surface sites, which may be beneficial for photocatalytic and antimicrobial applications (Fayed *et al*. 2025). The EDS spectrum (Fig. d) confirms the presence of Zn, O, and Se as the principal elements, verifying the successful formation of the SeO/ZnO nanocomposite.

The detected weight percentages were approximately Zn (41.5%), Se (32.2%), O (22.7%), and minor carbon content (3.6%), the latter likely originating from residual organic species or sample preparation. The elemental composition obtained from EDX analysis was used to estimate the molar ratios of Zn, Se, and O. Based on the measured weight percentages, the normalized atomic ratio was approximately Zn:Se:O ≈ 1.56:1:3.48, indicating a non-stoichiometric composition. This suggests that the synthesized material consists of a composite of ZnO and selenium oxide phases rather than a single uniform compound. The relatively high oxygen content may be attributed to oxide formation and surface-bound oxygen-containing groups from plant-derived biomolecules. The presence of selenium peaks alongside zinc and oxygen signals in the EDX spectrum confirmed the coexistence of these elements within the nanocomposite. However, this evidence does not allow definitive distinction between surface association and structural integration. The absence of impurity peaks suggests the relative purity of the synthesized material. Similar compositional observations have been reported in previous studies, where EDX analysis confirmed the presence of selenium within ZnO-based systems and its influence on optical and electronic properties (Thirupathi *et al*. 2024). The elemental composition suggests that Zn was predominantly present as ZnO, while selenium was most likely present in oxide form (SeO). The slight excess in oxygen content may be attributed to oxygen-containing functional groups from plant-derived biomolecules or minor experimental deviations, with

a possible minor contribution from selenium species in alternative oxidation states. Based on the elemental analysis and in the absence of direct crystallographic evidence, selenium is most likely present in oxide form (SeO), which is consistent with previously reported SeO/ZnO systems (Qanash *et al.* 2024), supporting the proposed composition and functionality of the nanocomposite.

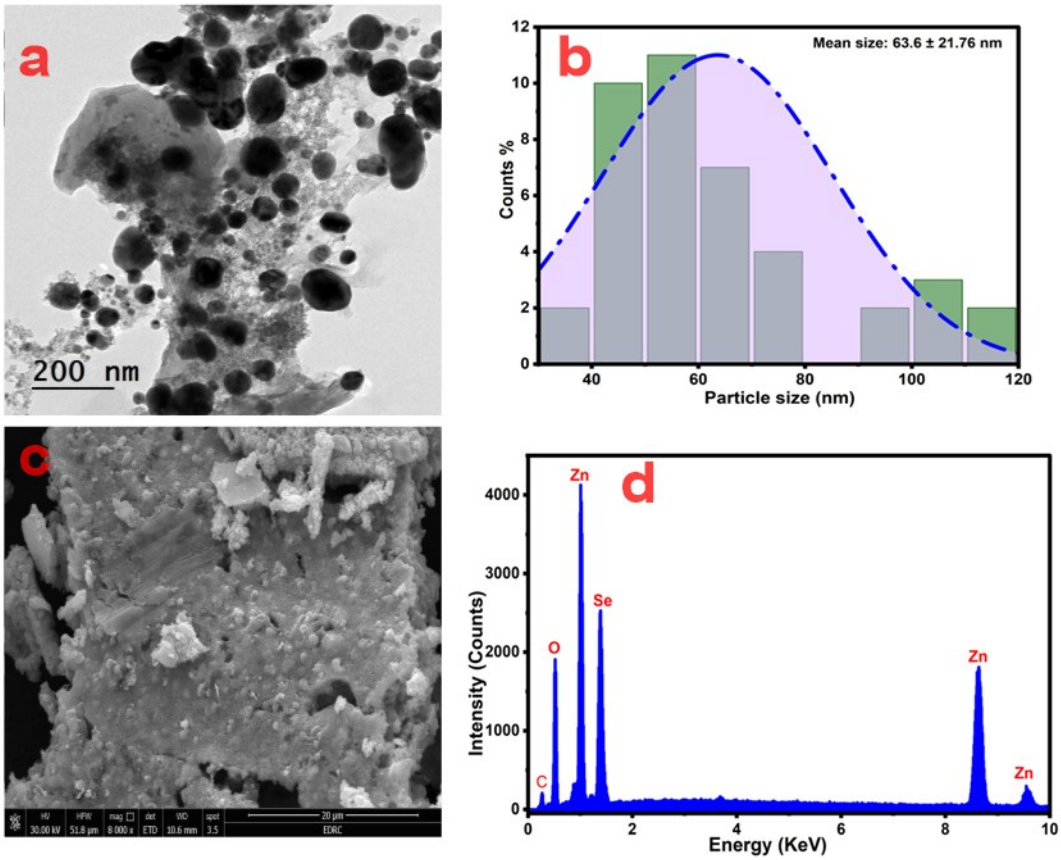

Fig. 2. Morphological and elemental characterization of green-synthesized SeO/ZnO nanocomposite: (a) TEM picture, (b) PSA histogram, (c) SEM micrograph, and (d) EDX spectrum with elemental composition analysis

Cytotoxicity and Cell Viability Assessment

The cytotoxic effect of SeO/ZnO NCs was evaluated against normal Vero cells and human lung carcinoma A549 cells over a concentration range of 15.8 to 1000 µg/mL, revealing a clear dose-dependent response (Fig. 3). Cell inhibition increased progressively with concentration, reaching 87.1% in Vero cells and 95.0% in A549 cells at 1000 µg/mL, while minimal cytotoxicity was observed at the lowest tested concentration (0.089% and 1.83%, respectively). Notably, A549 cells exhibited greater sensitivity across most concentrations; for instance, at 125 µg/mL, inhibition reached 55.30% in A549 cells compared with 21.7% in Vero cells, indicating differential susceptibility. The calculated IC_{50} values further confirmed this selectivity, with a significantly lower IC_{50} for A549 cells (101 µg/mL) compared to Vero cells (263 µg/mL), yielding a selectivity index of approximately 2.6. This preferential cytotoxicity toward cancer cells may be attributed to enhanced reactive oxygen species (ROS) generation induced by ZnO-based nanostructures, which disrupt mitochondrial function and trigger apoptosis, particularly in cancer cells that

already maintain elevated basal ROS levels (Almuhayawi *et al*. 2024; Alfattah *et al*. 2025). Additionally, selenium incorporation may contribute to redox modulation and pro-oxidant effects at higher concentrations, further promoting oxidative stress-mediated cell death pathways (Soliman and Salem 2025). The nanoscale particle size (63 nm) likely facilitated efficient cellular uptake, especially in rapidly proliferating tumor cells, enhancing intracellular interactions and cytotoxic efficacy (Amiri *et al*. 2025). Collectively, these findings demonstrate that SeO/ZnO nanocomposites exhibited concentration-dependent cytotoxicity with enhanced selectivity toward lung cancer cells.

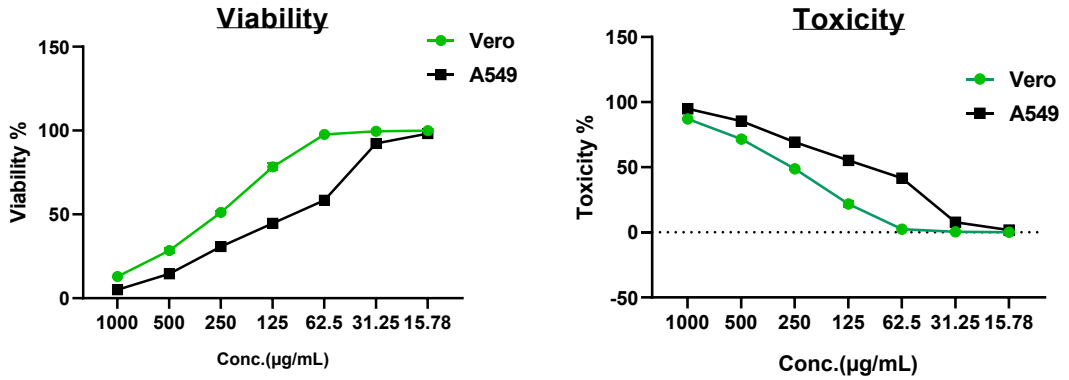

Fig. 3. Comparative evaluation of cytotoxicity and cell viability of SeO/ZnO nanocomposites in normal (Vero) and lung adenocarcinoma (A549) cell lines

Antibacterial Activity of SeO/ZnO NCs

The antibacterial performance of SeO/ZnO NCs was examined with respect to *E. coli* and *K. pneumoniae* as negative gram and *B. subtilis* as a positive gram using agar well diffusion MIC, MBC assays (Fig.4 and Table 1). The nanocomposite exhibited strong antibacterial activity in a strain-dependent manner. Among the tested bacteria, *B. subtilis* showed the greatest sensitivity, with both MIC and MBC values of 62.5 µg/mL, indicating a bactericidal effect at relatively low concentration. This was further supported by the largest inhibition zone (27.8 ± 0.75 mm), which exceeded that of the positive control (23.3 ± 0.61 mm). In contrast, *E. coli* demonstrated moderate sensitivity with 125 µg/mL and 250 µg/mL for MIC and MBC correspondingly with an inhibition zone of 20.1 ± 1.15 mm, notably higher than the positive control (13.07 ± 0.38 mm). *K. pneumoniae* exhibited comparatively lower susceptibility, with MIC and MBC values of 250 and 500 µg/mL, respectively, and an inhibition zone (19.2 ± 0.20 mm), which was close to that of the positive control (20.47 ± 0.15 mm). The MBC/MIC ratio was calculated to evaluate the antibacterial mode of action. A ratio ≤ 4 indicates bactericidal activity, confirming that the SeO/ZnO nanocomposite exhibited a bactericidal effect against the tested strains.

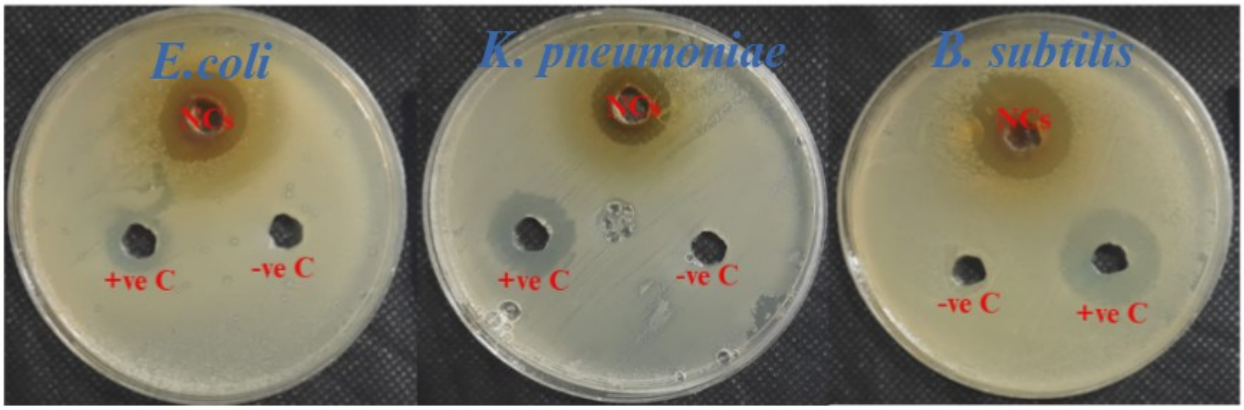

Fig. 4. Antibacterial activity of phytogenically synthesized SeO/ZnO NCs compared to the positive (+ve C) and negative (−ve C) control

Table 1. Antibacterial Activity of SeO/ZnO NCs against Tested Microbial Strains

Bacterial strain	MIC (µg/mL)	MBC (µg/mL)	Inhibition zone (mm) Mean ± SD	Positive control (mm) Mean ± SD
E. coli	125	250	20.1 ± 1.15	13.07 ± 0.38
K. pneumoniae	250	500	19.2 ± 0.20	20.47 ± 0.15
B. subtilis	62.5	62.5	27.8 ± 0.75	23.3 ± 0.61

The enhanced antibacterial performance, especially toward Gram-positive bacteria, is likely associated with structural disparities in the bacterial envelope. The thick peptidoglycan matrix of Gram-positive cells, devoid of an outer membrane, permits greater nanoparticle interaction and penetration. Conversely, the outer lipopolysaccharide membrane present in Gram-negative bacteria restricts nanoparticle permeability (Abdelghany *et al*. 2023). Compared with previously reported ZnO-based nanomaterials, the present SeO/ZnO nanocomposites exhibit competitive or superior antibacterial performance (Ifijen *et al.* 2022).

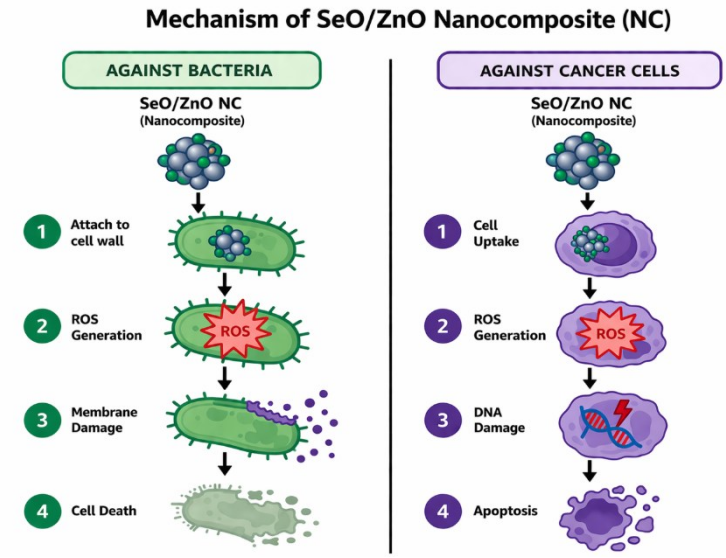

Fig. 5. Antibacterial and anticancer mechanisms of SeO/ZnO nanocomposite

It was demonstrated that selenium-functionalized metal oxide nanostructures significantly enhanced bactericidal efficiency due to improved redox activity and surface charge modulation (Selim *et al*. 2025). The larger inhibition zone observed against *B. subtilis* (27.8 mm) compared to the positive control further highlights the synergistic effect between selenium and ZnO in enhancing antimicrobial potency. The proposed antibacterial and anticancer mechanisms of the SeO/ZnO nanocomposite are illustrated in Fig. 5.

Comparative Antioxidant Assessment of SeO/ZnO NCs and Ascorbic Acid

The antioxidant capability of SeO/ZnO NCs was evaluated using DPPH and ABTS radical scavenging assays, demonstrating a clear concentration-dependent behavior (Fig. 6). In the DPPH assay, SeO/ZnO NCs exhibited 74.1% scavenging activity at 1000 µg/mL, in difference ascorbic acid achieved 95.7% at the same concentration. Similarly, in the ABTS assay, the nanocomposite achieved 65.9% inhibition at 1000 µg/mL compared to 96.0% for ascorbic acid. The calculated IC_{50} values further confirmed the antioxidant efficiency, with SeO/ZnO showing IC_{50} values of 257 µg/mL (DPPH) and 339 µg/mL (ABTS), whereas ascorbic acid demonstrated significantly lower IC_{50} values (43.6 and 47.3 µg/mL, respectively), reflecting its stronger radical scavenging capacity as a standard antioxidant. Although the nanocomposite exhibited lower activity than ascorbic acid, its antioxidant performance is comparable or superior to several previously reported zinc- or selenium-based nanomaterials (Mirzaei *et al*. 2021). Tettey and Shin (2019) reported that biologically synthesized ZnO nanoparticles exhibited a significant and concentration-dependent DPPH radical scavenging activity. The inhibition percentages increased progressively with concentration, reaching 48.8% at 125 µg/mL, 49.1% at 250 µg/mL, 49.5% at 500 µg/mL, and 56.1% at 1000 µg/mL, confirming the dose-responsive antioxidant behavior of ZnO nanoparticles (Tettey and Shin 2019).

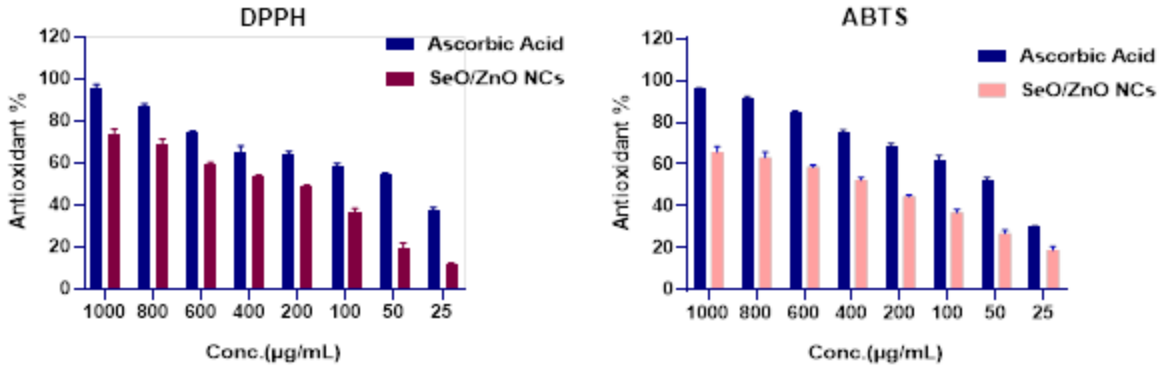

Fig. 6. Evaluation of antioxidant capacity through concentration-varied DPPH and ABTS tests of SeO/ZnO nanocomposites compared with ascorbic acid

CONCLUSIONS

1. The successful formation of SeO/ZnO nanocomposites was confirmed through comprehensive physicochemical characterization techniques, including UV–Vis, FTIR, TEM, and EDX analyses.

2. The SeO/ZnO NCs presented selective cytotoxic activity alongside A549 lung cancer cells (IC_{50} = 100.9 µg/mL) compared to normal Vero cells (IC_{50} = 63.5 µg/mL), indicating a favorable therapeutic selectivity.
3. The observed antibacterial activity of the SeO/ZnO nanocomposite may be attributed to the combined effects of Se and ZnO, as supported by previously reported studies on their individual biological activities.
4. The SeO/ZnO NCs showed concentration-dependent antioxidant endeavor in mutually DPPH plus ABTS assays, confirming its multifunctional redox-modulating capability.

ACKNOWLEDGMENTS

This work was funded by Princess Nourah bint Abdulrahman University Researchers Supporting Project number (PNURSP2026R62), Princess Nourah bint Abdulrahman University, Riyadh, Saudi Arabia.

REFERENCES

Abdelghany, T. M., Ganash, M. M., Alawlaqi, M. M., and Al-Rajhi, A. M. H. (2019). "Antioxidant, antitumor, antimicrobial activities evaluation of *Musa paradisiaca* L. pseudostem exudate cultivated in Saudi Arabia," *BioNanoScience* 9(1), 172-178. https://doi.org/10.1007/s12668-018-0580-x

Abdelghany, T. M., Al-Rajhi, A. M. H., Yahya, R., Bakri, M. M., Al Abboud, M. A., Yahya, R., Qanash, H., Bazaid, A. S., and Salem, S. S. (2023). "Phytofabrication of zinc oxide nanoparticles with advanced characterization and its antioxidant, anticancer, and antimicrobial activity against pathogenic microorganisms," *Biomass Conversion and Biorefinery* 13, 417-430. https://doi.org/10.1007/s13399-022-03412-1

Abdelghany, T. M., Al-Rajhi, A. M. H., Al Abboud, M. A., Alawlaqi, M. M., Ganash, M. M., Helmy, E. A. M., and Mabrouk, A. S. (2018). "Recent advances in green synthesis of silver nanoparticles and their applications: Future directions," *BioNanoScience* 8, 5-16. https://doi.org/10.1007/s12668-017-0413-3

Abdelhady, M. A., Abdelghany, T. M., Mohamed, S. H., and Abdelbary, S. A. (2024). "Impact of green synthesized zinc oxide nanoparticles for treating dry rot in potato tubers," *BioResources* 19(2), 2106-2119. https://doi.org10.15376/biores.19.2.2106-2119

Abu-Dalo, M., Jaradat, A., Albiss, B. A., and Al-Rawashdeh, N. A. (2019). "Green synthesis of TiO_2 NPs/pristine pomegranate peel extract nanocomposite and its antimicrobial activity for water disinfectiion," *Journal of Environmental Chemical Engineering* 7(5), article 103370. https://doi.org/10.1016/j.jece.2019.103370

Adrianto, N., Panre, A. M., Istiqomah, N. I., Riswan, M., Apriliani, F., and Suharyadi, E. (2022). "Localized surface plasmon resonance properties of green synthesized silver nanoparticles," *Nano-Structures & Nano-Objects* 31, article 100895. https://doi.org/10.1016/j.nanoso.2022.100895

Al-Rajhi, A. M. H., Yahya, R., Bakri, M. M., Yahya, R., and Abdelghany, T. M. (2022). "*In situ* green synthesis of Cu-doped ZnO-based polymers nanocomposite with

studying antimicrobial, antioxidant and anti-inflammatory activities," *Applied Biological Chemistry* 65, article 35. https://doi.org/10.1186/s13765-022-00702-0

Alfattah, M. A., Salem, S. S., Alharbi, H. M., Alwutayd, K. M., Albaqami, J. J., Zarah, R. K., Hamdi, H., and Soliman, M. K. Y. (2025). "Insight into phyto-fabrication of zinc oxide nanoparticles: GC-MS analysis, characterization, antibacterial, antioxidant and cytotoxic potentials against prostate and cervical carcinoma," *Bulletin of the Chemical Society of Ethiopia* 39. DOI.10.4314/bcse.v39i12.13

Alikhani, N., Hekmati, M., Karmakar, B., and Veisi, H. (2022). "Green synthesis of gold nanoparticles (Au NPs) using *Rosa canina* fruit extract and evaluation of its catalytic activity in the degradation of organic dye pollutants of water," *Inorganic Chemistry Communications* 139, article 109351. https://doi.org/10.1016/j.inoche.2022.109351

Almuhayawi, M. S., Alruhaili, M. H., Soliman, M. K. Y., Tarabulsi, M. K., Ashy, R. A., Saddiq, A. A., Selim, S., Alruwaili, Y., and Salem, S. S. (2024). "Investigating the *in vitro* antibacterial, antibiofilm, antioxidant, anticancer and antiviral activities of zinc oxide nanoparticles biofabricated from *Cassia javanica*," *PLoS One* 19, article e0310927. https://doi.org/10.1371/journal.pone.0310927

Amiri, Z., Shahbazi, S., Reiisi, S., Heidari, R., and Ghorbanpour, M. (2025). "Dual-loaded ZnO and Se nanoparticles in chitosan/alginate bio-composite: Synthesis, cytotoxicity, antioxidant activity, and anti-cervical cancer potential," *3 Biotech* 15, article 264. https://doi.org/10.1007/s13205-025-04436-w

Anitha, A., Ponmurugan, P., Natheer, S. E., Kannan, S., Sathishkumar, M., and Arunkumar, D. (2025). "Green synthesized Se@ZnO nanocomposites using *Ficus religiosa* extract for enhanced photocatalytic degradation of fast green dye and biological applications," *Materials Science and Engineering: B* 321, article 118478. https://doi.org/10.1016/j.mseb.2025.118478

Emaga, T. H., Andrianaivo, R. H., Wathelet, B., Tchango, J. T., and Paquot, M. (2007). "Effects of the stage of maturation and varieties on the chemical composition of banana and plantain peels," *Food Chemistry* 103, 590-600. https://doi.org/10.1016/j.foodchem.2006.09.006

Fayed, R. M., Baka, Z. A. M., Farouk, B. H., and El-Zahed, M. M. (2025). "Antibacterial and cytotoxic activities of a newly green synthesized ZnO/Se nanocomposite combined with *Washingtonia robusta* H. Wendl fruit extract," *Biocatalysis and Agricultural Biotechnology* 64, article 103500. https://doi.org/10.1016/j.bcab.2025.103500

Ifijen, I. H., Maliki, M., and Anegbe, B. (2022). "Synthesis, photocatalytic degradation and antibacterial properties of selenium or silver doped zinc oxide nanoparticles: A detailed review," *OpenNano* 8, article 100082. https://doi.org/10.1016/j.onano.2022.100082

Kadhim, R. J., Jabir, M. S., Sulaiman, G. M., Nayef, U. M., Mohammed, H. A., and Abomughaid, M. M. (2025). "The advancing of zinc oxide and gold nanoparticles as a promising therapeutic approach for future biomedical applications," *Plasmonics* 20, 10367-10388. https://doi.org/10.1007/s11468-025-03134-w

Khormi, M. A., Abdelglil, M. I., Alharbi, H. M., Alwutayd, K. M., Albaqami, J. J., Zarah, R. K., Hamdi, H., Alfattah, M. A., and Soliman, M. K. Y. (2025). "Unwrapping the phytofabrication of bimetallic silver–selenium nanoparticles: Antibacterial, anti-virulence (targeting *magA* and *toxA* genes), anti-diabetic, antioxidant, anti-ovarian and anti-prostate cancer activities," *Green Processing and Synthesis* 14, article 20250087. https://doi.org/10.1515/gps-2025-0087

Lashin, I., Hasanin, M., Hassan, S. A. M., and Hashem, A. H. (2023). "Green biosynthesis of zinc and selenium oxide nanoparticles using callus extract of *Ziziphus spina-christi*: Characterization, antimicrobial, and antioxidant activity," *Biomass Conversion and Biorefinery* 13, 10133-10146. https://doi.org/10.1007/s13399-021-01873-4

Majeed, A., Javed, F., Akhtar, S., Saleem, U., Anwar, F., Ahmad, B., Nadhman, A., Shahnaz, G., Hussain, I., and Hussain, S. Z. (2020). "Green synthesized selenium doped zinc oxide nano-antibiotic: Synthesis, characterization and evaluation of antimicrobial, nanotoxicity and teratogenicity potential," *Journal of Materials Chemistry B* 8, 8444-8458. https://doi.org/10.1039/D0TB01553A

Meenakshi, B., Ramanjaneyulu, E., Bharath, P., Gowri Sankar, M., and Ramachandran, D. (2024). "FT-IR studies and excess thermodynamic properties of binary mixtures at various temperatures and correlation with the Jouyban–Acree model," *Physics and Chemistry of Liquids* 62, 603-623. https://doi.org/10.1080/00319104.2024.2333957

Mirzaei, S. Z., Somaghian, S. A., Lashgarian, H. E., Karkhane, M., Cheraghipour, K., and Marzban, A. (2021). "Phyco-fabrication of bimetallic nanoparticles (zinc–selenium) using aqueous extract of *Gracilaria corticata* and its biological activity potentials," *Ceramics International* 47, 5580-5586. https://doi.org/10.1016/j.ceramint.2020.10.142

Nguyen, T. B. T., Ketsa, S., and Van Doorn, W. G. (2003). "Relationship between browning and the activities of polyphenol oxidase and phenylalanine ammonia lyase in banana peel during low temperature storage," *Postharvest Biology and Technology* 30, 187-193. https://doi.org/10.1016/S0925-5214(03)00103-0

Pasieczna-Patkowska, S., Cichy, M., and Flieger, J. (2025). "Application of Fourier transform infrared (FTIR) spectroscopy in characterization of green synthesized nanoparticles," *Molecules* 30, article 684. https://doi.org/10.3390/molecules30030684

Qanash, H., Bazaid, A. S., Alharazi, T., Barnawi, H., Alotaibi, K., Shater, A.-R. M., and Abdelghany, T. M. (2024). "Bioenvironmental applications of myco-created bioactive zinc oxide nanoparticle-doped selenium oxide nanoparticles," *Biomass Conversion and Biorefinery* 14, 17341-17352. https://doi.org/10.1007/s13399-023-03809-6

Rahman, A., Tan, A. L., Harunsani, M. H., Ahmad, N., Hojamberdiev, M., and Khan, M. M. (2021). "Visible light induced antibacterial and antioxidant studies of ZnO and Cu-doped ZnO fabricated using aqueous leaf extract of *Ziziphus mauritiana* Lam," *Journal of Environmental Chemical Engineering* 9, article 105481. https://doi.org/10.1016/j.jece.2021.105481

Ruiz-Duarte, E. V., Molina-Jiménez, J. P., Avila, D. A., Torres, C. O., and Horta-Piñeres, S. D. (2025). "Rapid synthesis of highly crystalline ZnO nanostructures: Comparative evaluation of two alternative routes," *Crystals* 15, article 640. https://doi.org/10.3390/cryst15070640

Saied, E., Doghish, A. S., Soliman, M. K. Y., El-Dakroury, W. A., Aloufi, A. S., Kiani, B. H., and Hashem, A. H. (2025). "Onion peel-mediated biosynthesis of TiO_2–ZnO bimetallic nanoparticles: Antimicrobial, antibiofilm and anticancer activities," *Electronic Journal of Biotechnology* 77, 12-23. https://doi.org/10.1016/j.ejbt.2025.06.001

Selim, S., Saddiq, A. A., Ashy, R. A., Baghdadi, A. M., Alzahrani, A. J., Mostafa, E. M., Al Jaouni, S. K., Elamir, M. Y. M., Amin, M. A., and Salah, A. M. (2025). "Bimetallic selenium/zinc oxide nanoparticles: Biological activity and plant

biostimulant properties," *AMB Express* 15, 1. https://doi.org/10.1186/s13568-024-01808-y

Selim, S., Soliman, M. K. Y., Almuhayawi, M. S., Alruhaili, M. H., Gattan, H. S., Saddiq, A. A., Hagagy, N., Alzahrani, A. J., Al Jaouni, S. K., and Salem, S. S. (2025). "Green synthesis, characterization, molecular simulation and *in vitro* biomedical application of magnesium oxide nanoparticles," *PLoS One* 20, article e0332367. https://doi.org/10.1371/journal.pone.0332367

Soliman, M. K. Y., Doghish, A. S., Hashem, A. H., Abdel-Maksoud, M., El-Dakroury, W. A., Alamri, A., Ebaid, H., Hasanin, M. S., and Saied, E. (2025). "Novel trimetallic (TiO_2–MgO–Au) nanoparticles: Biosynthesis, characterization, antimicrobial and anticancer activities," *Green Processing and Synthesis* 14, article 20250007. https://doi.org/10.1515/gps-2025-0007

Soliman, M. K. Y., Abu-Elghait, M., Salem, S. S., and Azab, M. S. (2024). "Multifunctional properties of silver and gold nanoparticles synthesis by *Fusarium pseudonygamai*," *Biomass Conversion and Biorefinery* 14, 28253-28270. https://doi.org/10.1007/s13399-022-03507-9

Soliman, M. K. Y., and Salem, S. S. (2025). "Uncovering the potential of biofabricated *Ananas comosus* peel selenium nanoparticles for antibacterial, antibiofilm, suppression of virulence genes (can and LuxS), anticancer and antioxidant properties," *BMC Biotechnology* 25, 1-21. https://doi.org/10.1186/s12896-025-00999-x

Someya, S., Yoshiki, Y., and Okubo, K. (2002). "Antioxidant compounds from bananas (*Musa cavendish*)," *Food Chemistry* 79, 351-354. https://doi.org/10.1016/S0308-8146(02)00186-3

Tettey, C. O., and Shin, H. M. (2019). "Evaluation of the antioxidant and cytotoxic activities of zinc oxide nanoparticles synthesized using *Scutellaria baicalensis* root," *Scientific African* 6, article e00157. https://doi.org/10.1016/j.sciaf.2019.e00157

Thirupathi, B., Pongen, Y. L., Kaveriyappan, G. R., Dara, P. K., Rathinasamy, S., Vinayagam, S., Sundaram, T., Hyun, B. K., Durairaj, T., and Sekar, S. K. R. (2024). "*Padina boergesenii* mediated synthesis of Se-ZnO bimetallic nanoparticles for effective anticancer activity," *Frontiers in Microbiology* 15, article 1358467. https://doi.org/10.3389/fmicb.2024.1358467

Upadhyay, R. K., Deshmukh, S., Saha, S., Barman, A., and Roy, S. S. (2015). "Optical, structural, catalytic and electrochemical properties of the Au nanoparticles synthesized using CTAB-based gels," *Journal of Materials Science: Materials in Electronics* 26, 7515-7522. https://doi.org/10.1007/s10854-015-3387-3

Article submitted: February 26, 2026; Peer review completed: March 29, 2026; Revised version received: April 1, 2026; Further revised version received: April 8, 2026; Accepted: April 12, 2026; Published: April 21, 2026.
DOI: 10.15376/biores.21.2.5010-5023